Numerical Simulation of Highly Buoyant Fluid at Supercritical Pressure

Yon-Yeong Bae [a*], Eung-Seon Kim[a], Minhwan Kim[a]
[a]*Korea Atomic Energy Research Institute, 111 Daedeok-daero 989, Yuseong, Daejeon, Korea 34057*
[*]*Corresponding author: yybae@kaeri.re.kr*

1. Introduction

Deterioration of heat transfer in an upward-flowing fluid in vertical tubes has long been an interesting but difficult subject since the introduction of supercritical pressure water as a heat transporting medium in fossil fuel power plants. The study of fluid-thermal behaviour under supercritical pressure either by experiment or numerical method is not simple and easy due to the drastic property variation shown in Figure 1.

As a supplementary means to experiments, numerical simulations were sought by many researchers to investigate what the mechanism behind the deterioration of heat transfer is for decades. However, not a single existing turbulence model was successful in reproducing the sudden temperature rise occurring at the heated tube wall, in which a buoyancy-influenced fluid flows upward against gravity.

In this paper, first, the derivation of Pr_{t-v} is briefly described, and the discussion of the damping length (A^+), which appears in the damping function in the low-Reynolds number turbulence model, is discussed. Then the results of numerical simulation using above-mentioned two critical factor are presented, and some conclusions will be drawn.

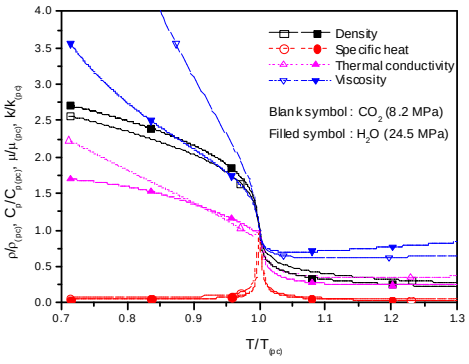

Figure 1. Variation of reduced properties of water and CO_2 with reduced pressure and temperature. Data from the NIST standard reference database [1]

2. Methods of Analysis

In this section the procedures of how the property-dependent Prandtl number, Pr_{t-v}, and relation between shear stress and damping length, A^+, were derived are described.

2.1 Property-dependent turbulent Prandtl number, Pr_{t-v}

Reynolds [2] reviewed more than thirty ways for predicting Pr_t and the Schmidt number (Sc_t) and showed that Pr_t may have some value far from unity. Kays [3] examined the then-available experimental data on Pr_t for a two-dimensional turbulent boundary layer; however, the examination was limited to cases with mild property variations. Pr_t has been treated as a constant of around 0.9 or unity in most earlier numerical works. However, there are many cases where Pr_t is far from unity.

Bae [4] suggested a new formulation of Pr_t by extending the Reynolds analogy and the behavior of turbulent boundary layer in a circular tube. The new formulation of Pr_t begins with revisiting the well-known Reynolds analogy, which implies the equality of diffusivity between momentum and heat transfer [5]. Having included the property variations as well as velocity and temperature in the procedure of deriving the ratio between turbulent momentum and energy transfer, the property-dependent Pr_t was derived as follows.

$$Pr_{t-v} = \frac{h_1 h_2 \left\{1 + \frac{\bar{u}}{\bar{\rho}}\left|\left(\frac{\partial \bar{\rho}}{\partial y}\right)\Big/\left(\frac{\partial \bar{u}}{\partial y}\right)\right|\right\}}{1 + \frac{\bar{T}}{\bar{\rho}}\left|\left(\frac{\partial \bar{\rho}}{\partial y}\right)\Big/\left(\frac{\partial \bar{T}}{\partial y}\right)\right| + \frac{\bar{T}}{\bar{c_p}}\left|\left(\frac{\partial \bar{c_p}}{\partial y}\right)\Big/\left(\frac{\partial \bar{T}}{\partial y}\right)\right|} \quad (1)$$

The functions h_1 and h_2 are added to make sure that the value of Pr_{t-v} approaches the asymptotic values at the two extremes; the wall and the centerline of a tube.

$$h_1 = 1 - e^{-y^+/A^+} \quad (2)$$

$$h_2 = 0.5\left[1 + tanh\left(\frac{B - y^+}{10}\right)\right] \quad (3)$$

The constant 10 in Eq. (3) is set as to make sure that the function h_2 varies smoothly around $y^+ = B$, and beyond that point the flow is in the wake region. The location of $y^+ = B$ is virtually outer edge of a turbulent boundary layer, so B was set as the y^+ value at $r = 0.8R$.

2.2 Shear stress under Buoyancy

2.2.1 Without velocity overshoot

First the case without velocity overshoot, which implies an appearance the local velocity peak (not the maximum) is presented.

In the low-Reynolds number turbulence model, the eddy viscosity is expressed as

$$\bar{\mu}_t = \bar{\rho}\bar{\nu}_t = \bar{\rho} C_\mu f_\mu \frac{\tilde{k}^2}{\tilde{\varepsilon}} \quad (4)$$

where the damping function f_μ is defined in the Myong-Kasagi model [6] as

$$f_\mu = \left[1 - e^{-y^+/A^+}\right]\left(1 + 3.45/Re_t^{1/2}\right) \quad (5)$$

The damping length, A^+, has been treated as a constant in most of earlier literature, but in this paper will be treated as a function of local shear stress.

Following the procedure taken by Cebeci [7] when he derived a relation between shear stress at the buffer layer and damping length, a similar relation was derived under an assumption that volume expansion due to density decrease (temperature increase) can be treated as wall mass suction.

When we treat the wall normal velocity as a constant related to the strength of buoyancy, the two-dimensional boundary-type momentum conservation equation in including buoyancy is written as

$$\frac{d\tau}{dy} - \frac{\rho v_w(x)\tau}{\mu} = (\rho - \rho_b)g \quad (6)$$

Although a flow in a tube is treated here, the equation was written in Cartesian coordinate, under an assumption of thin boundary layer.

The solution to Eq. (6) under boundary condition, $\tau = \tau_w$ at $y = 0$ is

$$\frac{\tau}{\tau_w} = \frac{\lambda(\rho_b - \hat{\rho})g\hat{\mu}}{\hat{\rho} v_w \tau_w}\left(1 - e^{\frac{\hat{\rho} v_w y}{\hat{\mu}}}\right) + e^{\frac{\hat{\rho} v_w y}{\hat{\mu}}} \quad (7)$$

The parameter λ in Eq. (7) was introduced to account for the variation of properties across the viscous sublayer and buffer layer, and will be treated as a function of buoyancy. The hat ($\widehat{\ }$) over the density and viscosity in Eq. (7) implies that those variables were average over the range $0 \le y^+ \le \delta$. When we use the definitions of Grashof number $\widehat{Gr}_b = \rho_b(\rho_b - \hat{\rho})gd^3/\mu_b^2$, the skin friction coefficient $C_f = 2\tau_w/\rho_b u_b^2$ and the Blasius correlation $C_f = K_1 Re_b^{-0.25}$ with $K_1 = 0.079$, the term in front of the tall parenthesis on the right-hand side of Eq. (7) can be straightforwardly rewritten as a combination of dimensionless parameters as,

$$\frac{\lambda(\rho_b - \hat{\rho})g\hat{\mu}}{\hat{\rho} v_w \tau_w} = \frac{\lambda}{v_w^+} B$$
$$B = \frac{\lambda}{v_w^+}\left(\frac{2}{K_1}\right)^{3/2} \frac{\widehat{Gr}_b}{Re_b^{2.625}}\left(\frac{\hat{\mu}}{\mu_b}\right)\frac{\rho_b^{1/2}\rho_w^{1/2}}{\hat{\rho}} \quad (8)$$

Noting $\hat{\rho} v_w \delta_t/\hat{\mu} = v_w^+ \delta_t^+$ and that v_w is of order of the local value of $(\rho - \rho_o)g\mu/\rho\tau$, Eq. (7) can be written a further simplified form

$$\frac{\tau_{\delta_t}}{\tau_w} = \lambda - (\lambda - 1)e^{B\delta_t^+} = f_1 \quad (9)$$

Eq. (9) represents shear stress at the buffer layer in the absence of velocity overshoot (in other words M-shape velocity profile).

Since we know from Eq. (9) that only independent variable is $B\delta_t^+$ it should not be unreasonable to assume that λ also depends on $B\delta_t^+$. The function λ shows asymptotic behaviours in the two extremes: the forced convection limit $B\delta_t^+ = 0$; and the boundary between mixed and natural convection $B\delta_t^+ = B^*\delta_t^+$. After conducting an extensive numerical trial and error process against the experimental data, the constants a, b, c and d were determined and the following dependences of λ on $B\delta_t^+$ were developed.

$$\lambda_{CO_2} = 1 + 2 \cdot \left[1 + \tanh\left(\frac{B\delta_t^+ - 0.2}{0.1}\right)\right] \quad (10)$$

$$\lambda_{water} = 1 + 4 \cdot \left[1 + \tanh\left(\frac{B\delta_t^+ - 0.2}{0.1}\right)\right] \quad (11)$$

2.2.2 With velocity overshoot

When there appears a velocity overshoot, things become totally different, since the core flow (enclosed by the locus of the overshoot) will move forward with no or negligible interaction with the wall layer (the layer between the locus of the overshoot (wall layer) and the wall) as noted earlier by Hall [8]. In this case the convection terms was assumed to be negligibly small and the shear stress depends only on buoyancy. The governing equation simplifies to

$$\frac{d\tau}{dy} = -(\rho_b - \rho)g \quad (12)$$

By integrating Eq. (12) over the range $\delta_{t,o} \le y \le \delta_t$ we obtain

$$\frac{|\tau_{\delta_t}|}{\tau_w} = B\left(\delta_t^+ - \delta_{t,o}^+\right) = B\delta_t^+\left(1 - \frac{\delta_{t,o}^+}{\delta_t^+}\right) \quad (13)$$

From DNS data [9] and numerical experiment $\delta_{t,o}^+/\delta_t^+$ was estimated as a constant of 0.4. Then Eq. (13) becomes

$$\frac{|\tau_{\delta_t}|}{\tau_w} = 0.4B\delta_t^+ = f_2 \quad (14)$$

Eqs. (9) and (14) describes the shear stress at the buffer layer in the case of without and with velocity overshoot, respectively, and are shown in

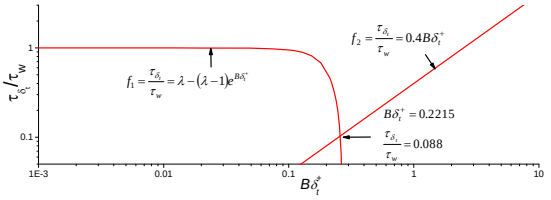

Figure 2. Graphical representation of Eqs. (9) and (14)

.

2.3 Shear stress as a function of damping length, A^+

2.3.1 Without velocity overshoot

In Cebeci's analysis [7] the damping length ratio, A^+/A_0^+, was proportional to $\left(\tau_{\delta_t}/\tau_w\right)^{-1/2}$, but the numerical works performed by the authors indicated that A^+/A_0^+, was proportional to $\left(\tau_{\delta_t}/\tau_w\right)^{1/2}$. The reason for this discrepancy might be explained by the fact that the shear stress in our case is associated with a negative v_w^+ (suction at the wall) instead of positive v_w^+ in the Cebeci's analysis. In the absence of a pressure gradient τ_{δ_t}/τ_w exponentially decreases with buoyancy strength $B\delta_t^+$ as can be seen in Figure 2, before the appearance of velocity overshoot or natural convection picks up. Finally the relation between the damping length and the shear stress at the buffer layer is expressed as follows.

$$\frac{A^+}{A_0^+} = \left(\frac{\tau_{\delta_t}}{\tau_w}\right)^{1/2} \tag{15}$$

2.3.2 With velocity overshoot

As discussed in the earlier section, once a velocity peak appears, the two flow fields separated from each other by the peak no longer depend on each other. Therefore, Eq. (15) is no longer valid when a velocity overshoot appears within the range of $0 \le y \le \delta_t$. Recalling 70 as the typical value of A^+ under no buoyancy, and the value of y^+ at the edge of the turbulent boundary layer being within the range of 200 – 300 , it is reasonable to assume the value of A^+ to be 30% of the value of y^+ at $\partial u/\partial y = 0$, y_o^+, [10] resulting in the following simple equation. However, the value of 30% would asymptotically converge to 100% as y_o^+ approaches zero. Thus, the following equation for A^+ in this flow regime is introduced.

$$A^+ = \gamma y_o^+ \tag{16}$$

The function γ take values that change between 0.3 and 1.0 in a continuous and gradual manner. The value of A^+ should be confined within the range of $5 < A^+ < 70$ as long as the Myong-Kasagi model is used. Noting that an asymptotic behaviour can be best described by a hyperbolic function, the following equation for γ is introduced.

$$\gamma = 0.3 + 0.35\left[1 + \tanh\left(\frac{100 - y_o^+}{50}\right)\right] \tag{17}$$

The constants 50 and 100 in Eq. (17) were tuned to the KAERI's experimental data obtained with CO_2 as a medium, and might be different for other mediums. Eq. (17) was formulated such that it results in $A^+ = y_o^+$ when y_o^+ is far smaller than 70 and $A^+ = 0.3y_o^+$ when y_o^+ is far greater than 70.

Table 1 summarizes the proposed procedure for determining A^+.

Table 1 Summary of procedure for determining A^+

Condition	A^+
$B\delta_t^+ < B^*\delta_t^+$	$Minimum\ of\left(A_o^+ f_1^{1/2}, \gamma y_o^+\right)$
$B\delta_t^+ > B^*\delta_t^+$	$Minimum\ of\left(A_o^+ f_2^{1/2}, \gamma y_o^+\right)$
• $\delta^+ = 30$ for $y_o^+ \ge 30$ $\delta^+ = y_o^+$ for $11.8 < y_o^+ < 30$ and $\delta^+ = 11.8$ for $y_o^+ \le 11.8$, • $\delta_t^+ = \delta^+/\overline{Pr}^{0.4}$, γ : Eq. (17) • A^+ is bounded by $5 \le A^+ \le 70$ • $B^*\delta_t^+ = 0.2215$ for $\gamma = 3$.	

4. Results

The numerical method are described in [11] and will not be repeated.

The results of numerical simulations are presented for the two cases summarized in Table 2.

Table 2. Flow conditions at the inlet for the cases studied (all upward flow)

Cases	Fluid	P (MPa)	G (kg/m²s)	q (kW/m²)	*d* mm
Case 1 [12]	Water	24.5	380	410	10.4
Case 3 [13]	CO_2	7.75	200	38	4.57

Figure 3 shows the axial distribution of T_w for Case 1. The introduction of both A^+ and Pr_{t-v} into the numerical simulation evidently resulted in extremely good agreement with the experimental data. The temperature peak was quite accurately captured with the right value at the right location. The numerical results demonstrated the appropriateness of functional dependence of A^+ on the buoyancy parameter, $B\delta_t^+$.

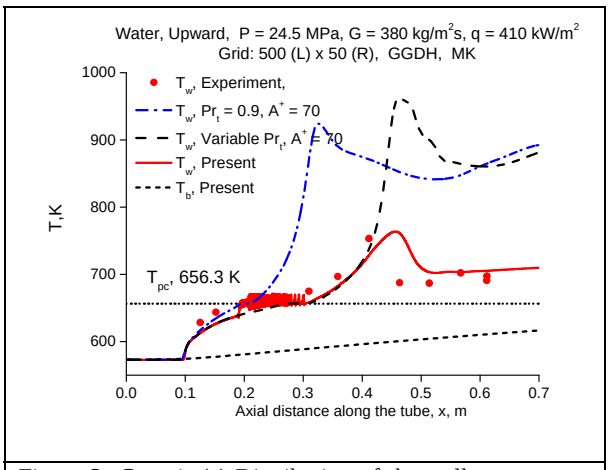

Figure 3 Case 1. (a) Distribution of the wall temperature along the tube

As is evident in Figure 4, the introduction of A^+ greatly improved the numerical performance in Case 2, showing a capability of capturing the two temperature

peaks at the correct positions with striking precision. The conventional method (dash dot) largely overestimates the experimental data. The introduction of Pr_{t-v} only slightly improved, but still show overestimation.

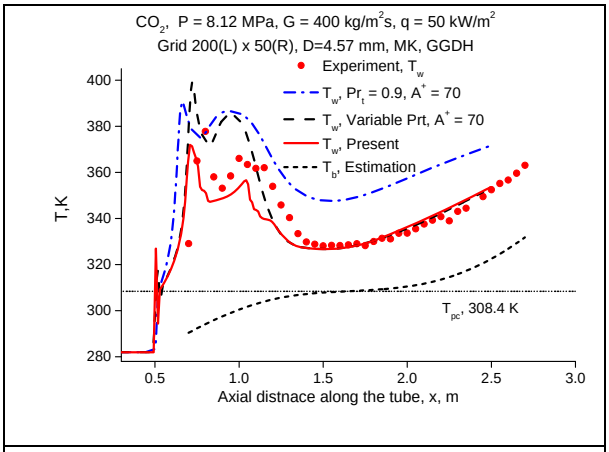

Figure 4 Case 3. (a) Distribution of the wall temperature along the tube.

3. Conclusions

The damping length, A^+, is believed to be an important parameter in the turbulent boundary layer controlling the behavior of the buffer layer, where most turbulence is generated. Under the assumption that the value of A^+ will change in accordance with the strength of buoyancy, a functional relation between A^+ and the shear stress at the edge of the thermal boundary layer, τ_{δ_t}, was established by directly integrating the momentum equation under some appropriate assumptions. Incorporating A^+ as a function of τ_{δ_t}, as well as Pr_{t-v} previously proposed by Bae [4] in the RANS type numerical calculations of fluid flows under strong property variations accompanying consequential heat transfer deterioration, resulted in excellent agreement with the experimental data. In particular, the temperature peaks and plateaus were also quite accurately captured.

The authors hope the method proposed in this paper will provide the research groups working in this field with a reasonable numerical tool for RANS type calculations.

REFERENCES

[1] E. W. Lemmon, M.L. Huber, M.D. McLinden, Reference Fluid Thermodynamics and Transport Properties. NIST Standard Reference Database 23, Version 9.0, 2010.

[2] A.J. Reynolds, The prediction of turbulent Prandtl and Schmidt numbers, Int. J. Heat and Mass Transfer Vol. 18 pp. 1055-1069, 1975.

[3] W.M. Kays, Turbulent Prandtl number-Where are we, Journal of Heat Transfer, Vol. 116, pp. 284-295, 1994.

[4] Y. Y. Bae, A new formulation of variable turbulent Prandtl number for heat transfer to supercritical fluids with strong property variation, Int. J. Heat and Mass Transfer, Vol. 92, pp. 792-806, 2016.

[5] W. Kays, M. Crawford, B. Weigand, Convective Heat and Mass Transfer, 4th ed., McGraw Hill International Edition, P. 231. 2005.

[6] H. K. Myong, N. Kasagi, A new approach to the improvement of k–ε turbulence model for wall bounded shear flows, JSME International Journal, Vol. 33, pp. 63–72, 1990.

[7] T. Cebeci, Behavior of Turbulent Flow near a Porous Wall with Pressure Gradient, AIAA J. 8 (12) (1970) 2152-2156.

[8] W. B. Hall, "Heat Transfer near the Critical Point," Advances in Heat Transfer, Ed. J. P. Harnett and T. F. Irvine, Vol. 7 (1971) 1-86.

[9] J. H. Bae, J. H. Yoo, H. Choi, "Direct numerical simulation of turbulent supercritical flows with heat transfer," Physics of Fluids 17 105104 (2005).

[10] J. A. Schetz, Boundary Layer Analysis, Prentice Hall, Englewood Cliffs, New Jersey, 1993. p. 340.

[11] Y. Y. Bae, E. S. Kim, M. H. Kim, Assessment of low-Reynolds number k-ε turbulence models against highly buoyant flows, Int. J. Heat and Mass Transfer. 108 (2017) 529-536..

[12] G. V. Alekseev, V. A. Silin, A. M. Smirnov, V. I. Subbotin, "Study of the thermal conditions on the wall of a pipe during the removal of heat by water at a supercritical pressure," Translated version of Teplofizika Vysokith Temperatur 14(4) (1976) 769-774.

[13] Y. Y. Bae, Mixed convection heat transfer to carbon dioxide flowing upward and downward in a vertical tube and an annular channel, Nuclear Engineering and Design, Vol. 241 pp. 3164– 3177, 2011.